ACS Chemical Neuroscience

Article

Discovery of novel pyrazolopyrimidinone derivatives as PDE9A inhibitors capable of inhibiting BuChE for treatment of Alzheimer's disease

Yan-Fa Yu, Ya-Dan Huang, Chen Zhang, Xu-Nian Wu, Qian Zhou, Deyan Wu, Yinuo Wu, and Hai-Bin Luo

ACS Chem. Neurosci., **Just Accepted Manuscript** • DOI: 10.1021/acschemneuro.7b00268 • Publication Date (Web): 07 Aug 2017

ACS Publications

ACS Chemical Neuroscience is published by the American Chemical Society. 1155 Sixteenth Street N.W., Washington, DC 20036

Discovery of novel pyrazolopyrimidinone derivatives as PDE9A inhibitors capable of inhibiting BuChE for treatment of Alzheimer's disease

Yan-Fa Yu[‡,a] Ya-Dan Huang[‡,a] Chen Zhang,[a] Xu-Nian Wu,[a] Qian Zhou,[a] Deyan Wu,[a]

Yinuo Wu[a,*] and Hai-Bin Luo[a,b,*]

[a] School of Pharmaceutical Sciences, Sun Yat-Sen University, Guangzhou 510006, PR China

[b] Collaborative Innovation Center of High Performance Computing, National University of Defense Technology, Changsha 410073, China

[‡]These authors contributed equally.

KEYWORDS: Phosphodiesterases 9 (PDE9), Butyrylcholinesterase (BuChE), Multi-target-directed ligands, Alzheimer's disease

ABSTRACT: Discovery of multi-target-directed ligands (MTDLs) targeting at different factors simultaneously to control the complicated pathogenesis of Alzheimer's disease (AD), has become an important research area in recent years. Both PDE9A and BuChE inhibitors could participate in different processes of AD to attenuate neuronal injuries and improve cognitive impairments. However, research on the MTDLs combining the inhibition of PDE9A and BuChE simultaneously has not been reported yet. In this study, a series of novel pyrazolopyrimidinone-rivastigmine hydrids were designed, synthesized, and evaluated *in vitro*. Most compounds exhibited remarkable inhibitory activities against both PDE9A and BuChE. Compounds **6c** and **6f** showed the best IC_{50} values against PDE9A (**6c**: 14 nM, **6f**:17 nM, respectively) together with the considerable inhibition against BuChE (IC_{50}, **6c**: 3.3 μM, **6f**: 0.97 μM). Their inhibitory potencies against BuChE were even higher than the anti-AD drug rivastigmine. Worthy to mention is that both showed moderate selectivity for BuChE over AChE. Molecular docking studies revealed their binding patters and explained the influence of configuration and substitutions on the inhibition of PDE9A and BuChE. Furthermore, compounds **6c** and **6f** exhibited negligible toxicity, which made them suitable for the further study of AD *in vivo*.

1. Introduction

Alzheimer's disease (AD) is an age-related neurodegenerative disorder, which is characterized by progressive memory loss, decline in language skills, and cognitive dysfunction.[1] In the report by Alzheimer's association (USA) in 2016,[2] AD has already become the third cause of death after cardiovascular diseases and cancer. About 46.8 million people worldwide are currently suffering from AD and about 10 million new cases were diagnosed in 2015. The number will rise to 131 million by 2050. The global cost for medication and care in AD patients was about $818 billion in 2015, which will rise to $1,000 billion in 2018 and $2,000 billion in 2030, respectively, bringing heavy economic burden to society and families.

The pathogenesis of AD is complicated and still not fully understood yet.[3] Low level of neurotransmitter acetylcholine (ACh) has been regarded as one of the main reasons for cognitive and memory impairments of AD patients.[4] Acetylcholinesterase inhibitors (AChEIs) could inhibit acetylcholinesterase (AChE) reversibly or irreversibly, increasing the concentration of ACh in brain to improve cognitive impairments. Currently, three out of four drugs approved by FDA in AD therapies are AChEIs (donepezil, rivastigmine, and galantamine).[5] However, the concentration of AChE would fall to 10-15% in advanced AD patients, which made selective AChEIs work not as efficient as that in the early stage. Butyrylcholinesterase (BuChE) is the other major form of cholinesterases, the inhibition of which could also improve the levels of ACh. Compared to low level of AChE in AD advanced stage, the concentration of BuChE remained the same or even increased up to 2-fold.[6] Now, dual inhibitors of AChE and BuChE or selective BuChE inhibitors have been considered as new therapeutic strategies for AD patients, especially for those in the advanced stage.[7]

Phosphodiesterases 9 (PDE9), belonging to the phosphodiesterase (PDE) super family of enzymes, could hydrolyze the intracellular second messenger cyclic guanosine monophosphate (cGMP) specifically with the highest affinity among all the 11 PDE subfamilies.[8] PDE9A is the only isoform of

PDE9, which is highly expressed in the cortex, basal ganglia, hippocampus, and cerebellum of brain. The inhibition of PDE9A could decrease the concentration of cGMP in brain to active NO/cGMP/PKG/CREB signaling, increasing the level of brain-derived neurotrophic factor (BDNF), restoring proteins associated with memory and attenuating neuronal injuries in hippocampal area. Thus, PDE9 has been regarded as a novel and promising therapeutic target for AD.[9] PDE9 inhibitors **BAY 73-6691** and **PF-04447943** could improve memory performance in several rodent memory tasks including social recognition and object recognition tasks, Morris water maze and *etc*.[10,11] Compared with AChE inhibitor donepezil, PDE9 inhibitor **BAY 73-6691** could not only prolong both early and late long-term potentiation (LTP) in hippocampal slices, but also transform early LTP into late LTP.[12] In the APP transgenic Tg2576 mice, **BAY 73-6691** could restore $A\beta_{42}$ oligomers induced LTP and **PF-04447943** could regulate dendritic spine density in hippocampal neurons.[13,14] Furthermore, **BAY 73-6691** could protect $A\beta_{25-35}$ induced oxidative damage in hippocampus and attenuate damage in hippocampal neurons.[15] Currently, PDE9 inhibitors **BI-409306** and **PF-04447943** are subjected to AD clinical trials.

Based on the multifactorial nature of AD, multi-target-directed ligands (MTDLs), single compounds which target at different enzymatic systems or receptors involved in AD simultaneously, attracted widespread attention in recent years, and thus numerous MTDLs were developed.[16-17] The pharmacophores of current anti-AD drugs such as donepezil and rivastigmine were often used in the discovery of MTDLS with cholinesterase inhibitory activities. Several efficient ones such as ladostigil and memoquin have been proved to be active in preclinical or even clinical trials.[18,19]

On the other hand, an *in vivo* study demonstrated that co-administration of PDE4 inhibitor roflumilast and AChE inhibitor donepezil could fully reverse scopolamine-induced memory deficit in the objective recognition task, while single administration of each drug could not.[20] A clinical study showed that both AChE inhibitor galantamine and PDE3 inhibitor cilostazol monotherapy increased cognitive, affective, and activities of daily living functions in AD patients and the combination of them gave better effect

than the monotherapy. [21] All these results indicated that controlling the PDE inhibition and ChE inhibition simultaneously may have better results than single one. However, multi-target-directed ligand combining the inhibition of PDEs and ChE simultaneously has not been reported yet.

Aiming at discovery of multi-target-directed ligands combining dual inhibitory activities of PDE9A and ChE, a series of novel pyrazolopyrimidinone-rivastigmine hydrids were designed and synthesized in this study. The inhibition of PDE9A, AChE, and BuChE were evaluated in *vitro*. The antioxidant activity and toxicity were also assessed. Molecular docking and dynamics simulations were used to explore binding modes and underlying mechanisms of lead compounds with enzymes, providing evidence for further structural modifications.

2. Result and discussion

2.1. Rational design of PDE9A inhibitors capable of inhibiting ChE.

We used to report an efficient PDE9A inhibitor **C33**, which showed IC_{50} of 16 nM against PDE9A and exhibited good pharmacokinetic properties.[22] Experiments *in vivo* demonstrated that **C33** has memory improving effect on learning and memory dysfunction animal model induced by scopolamine or $A\beta_{1\text{-}42}$. From the X-ray crystal structure of the **C33**-PDE9A complex, below information was obtained. **C33** formed a hydrogen bond with Gln453 and an aromatic π-π stack against Phe456 *via* its pyrazolopyrimidinone scaffold (Figure 1). As Gln453 and Phe456 are two conservative residues in the binding pocket of PDE9A, the interactions with them are important for the affinity of inhibitors with PDE9.[23-25] Thus, pyrazolopyrimidinone motif was kept as the scaffold of our designed compounds for their potency with PDE9A.

Among current AChEI drugs approved for AD, rivastigmine is the only one inhibiting both AChE and BuChE simultaneously.[26] Clinical studies proved that mild to moderately severe AD patients treating with rivastigmine have apparent ameliorative changes in the brain.[27] This result is in concert

with the hypothesis that inhibition of both AChE and BuChE may have neuroprotective and disease-modifying effects in the advanced AD patients. According to the crystal structures of the AChE-rivastigmine and BuChE-rivastigmine complexes, the carbamate moiety of rivastigmine linked to the active-site serine of cholinesterase covalently, which is the pharmacophore for its potency against AChE and BuChE.[28]

Based on these evidences, a series of novel pyrazolopyrimidinone-rivastigmine hydrids were designed, which comprised of pyrazolopyrimidinone and carbamate moiety in one molecule. The phenylethylamine motif, existing in the structure of both **C33** and rivastigmine, was used as part of the linker according to drug fusion principle (Figure 1).

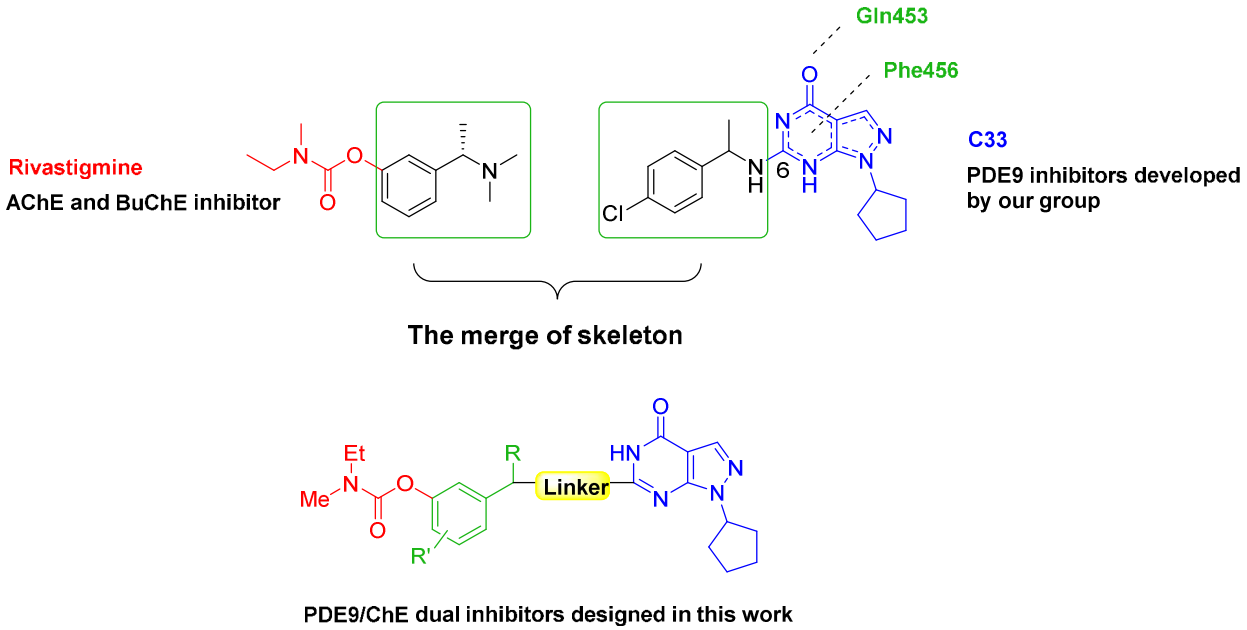

Figure 1. Rational design of PDE9 inhibitors capable of inhibiting ChE.

2.2. Chemistry

The synthetic route of compounds **6a-6f** was outlined in Scheme 1.[22,24] The starting material trichloropyrimidine (**1**) could be obtained in high yield by the Vilsmeier-Haack reaction of barbituric acid in the presence of phosphorus oxychloride. The pyrazole ring of compound **1** was then closed by

reaction with cyclopentyl hydrazine (**2**), giving the pyrazolo[3,4-d]pyrimidine **3**. Hydrolysis of compound **3** by KOH afforded the pyrazolo[3,4-d]pyrimidin-4-one **4.** Subsequently, compound **4** reacted with corresponding amines to yield the series of compounds **5** in good yields. The carbamoylation of compounds **5a-5e** with the *N, N*-ethyl(methyl)carbamic chloride or *N, N*-dimethylcarbamic chloride in DMF with the assistance of NaH led to the designed compounds **6a-6f**.

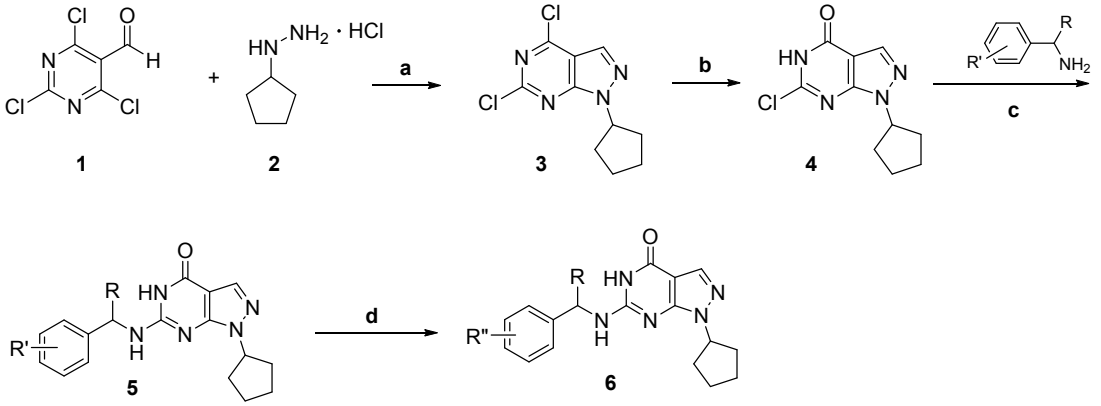

5a, R=H, R'=3-OH
5b, R=H, R'=3-OH,4-OMe
5c, R=H, R'=3-OMe,4-OH
5d, R=(*R*)-Me, R'=3-OH
5e, R=(*S*)-Me, R'=3-OH

6a, R=H, R''=3-OC(O)NEtMe
6b, R=H, R''=3-OC(O)NEtMe,4-OMe
6c, R=H, R''=3-OMe,4-OC(O)NEtMe
6d, R=(*R*)-Me, R''=3-OC(O)NEtMe
6e, R=(*S*)-Me, R''=3-OC(O)NEtMe
6f, R=H, R''=3-OMe,4-OC(O)NMe_2

Scheme 1. Reagents and conditions: (a) Triethylamine, -78 ^{o}C, THF; (b) 2N KOH, 60 ^{o}C; (c)Amine, *i*-PrOH, Triethylamine, reflux; (d) *N, N*-ethyl(methyl)carbamic chloride or *N, N*-dimethylcarbamic chloride, NaH, DMF, r.t.

The synthetic route of **13a-13b** is outlined in Scheme 2.[29] The condensation of 2-(methoxymethylene)malononitrile (**7**) with cyclopentylhydrazine (**8**) provided intermediate **9** in the presence of triethylamine. The intermediate **9** was then hydrolyzed with ammonium hydroxide and hydrogen peroxide to obtain intermediate **10.** And then, intermediate **10** reacted with (*R*)-ethyl-2-(((benzyloxy)carbonyl)amino)propanoate in the next step to give compound **11** under basic condition. Compound **11** was then hydrogenated with Pd/C to remove the Cbz group, providing intermediate **12** in

high yield. Compounds **13a** and **13b** were prepared in good yields by reaction of the corresponding aldehydes and sodium borohydride.

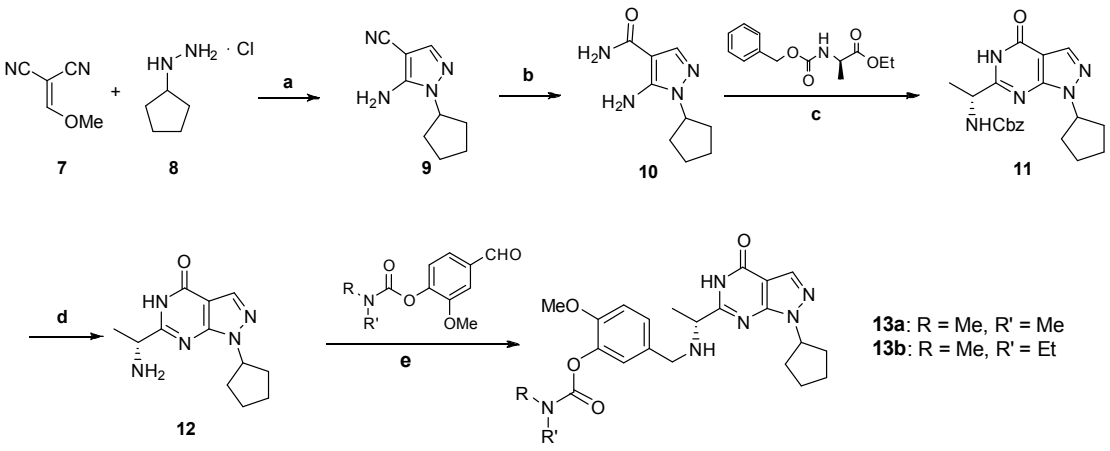

Scheme 2. Reagents and conditions: (a) Triethylamine, 0 °C, EtOH; (b) $NH_3 \cdot H_2O$, H_2O_2, EtOH, r.t.; (c) (*R*)-ethyl-2-(((benzyloxy)carbonyl)amino)propanoate, 60% NaH, dry THF, r.t.; (d)Pd/C, MeOH, H_2; (e) *i*-PrOH, $NaBH_4$, r.t.

2.3. The inhibitory activities of target compounds towards PDE9A *in vitro*

The inhibitory activities of compounds **6a-6f** against PDE9A were determined by bioassay with the same protocol as our previous reported work.[30] As compounds **5a-5e** have the pyrazolopyrimidinone scaffold, the inhibitory activities of compounds **5a-5e** against PDE9 were also evaluated. **Bay 73-6691** was used as the reference compound for the bioassay (IC_{50} = 51 nM).[31] The results were summarized in Table 1.

As expected, most designed compounds were potent PDE9A inhibitors. In the series of compounds **5**, with the hydroxyl group at the 3 or 4 position on the phenyl ring, the IC_{50} values against PDE9A ranged from 13 to 69 nM. Compound **5b** with 3- hydroxyl-4-methoxy groups and compound **5c** with 3-methoxy-4-hydroxyl groups substituted on the phenyl ring, gave comparable IC_{50} values of 39 and 35 nM respectively, while compound **5a** with only a hydroxyl group gave a slight lower IC_{50} of 53 nM. In our previous study, **C10** with no substituted group and **C33** with 4-chloro substituted on the phenyl ring

gave the IC_{50} values of 39 nM and 16 nM, respectively.[22] Combined with these data, we concluded that the properties of substitutions at phenyl nucleus would affect the inhibitory activities against PDE9A but not significantly. Compared with compound **5a**, compound **5d** with a methyl group at the R position gave the best IC_{50} (13 nM) among all the compounds in series 5, indicating that the steric hinderance has important effect on the affinity of compounds with PDE9A. However, compound **5e,** the stereoisomer of **5d** with different configuration, gave the IC_{50} of 69 nM against PDE9A. This difference in inhibitory activities caused by configuration also occurred on the two stereoisomers of **C33** but with totally contrary results. The *S*-isomer of **C33** gave better IC_{50} value (11 nM) than *R*-isomer (58 nM). The crystal structure of the **C33**-PDE9 complex revealed that the chlorophenyl tail of (*S*)-**C33** interacted with a small hydrophobic pocket while that of (*R*)-**C33** pointed out the molecular surface. The slightly better binding affinity of (*S*)-**C33** may come from more van der Waals interactions in the hydrophobic pocket. As the major structural difference among **C33**, **5d**, and **5e** is the hydroxyl group on the phenyl ring, we concluded that the hydroxyl group of **5d** and **5e** might form additional interactions with residues in the binding pocket of PDE9A, leading to the different inhibitory activities of **5d** and **5e**.

In the series of compounds **6,** with carbamate attaching on the hydroxyl group of compounds **5**, the results were quite different from structure-activity relationship (SAR) of **5**. Compound **6c**, with 3-methoxyl and 4-carbamate groups on the phenyl ring, gave the best IC_{50} of 14 nM. Compound **6a** with 3-carbamate group gave a comparable IC_{50} against PDE9A (IC_{50}: 19 nM). The two stereoisomers **6d** and **6e** with different configurations, gave the IC_{50} of 37 nM and 30 nM, respectively. It seemed that the difference in inhibitory activities of the two stereoisomers **5d** and **5e** disappeared after the carbamate groups attaching on the hydroxyl group of **5**. This result further supported our speculation that the hydroxyl group of compounds **5d** and **5e** may form additional interactions with PDE9A. Furthermore, as the volume of *N, N*-ethylmethylcarbamate group is relative large, we speculated that the attachment of this group on compounds **6a-6f** might affect spatial orientation of phenyl group**,** resulting in the

difference in affinity with PDE9A. Compound **6f,** with a *N, N*-dimethylcarbamate group was also synthesized and evaluated for the comparison with compound **6c**. The IC_{50} of compound **6f** against PDE9A was 17 nM, which was almost the same with compound **6c**. Compounds **13a** and **13b** with different linkers were also designed and synthesized. However, both of them showed low inhibition against PDE9A at 100 nM. We concluded that the size of linker used in compounds **13a** and **13b** might be too large to fit well in the binding pocket of PDE9A for high affinity.

2.4. The inhibitory activities of target compounds towards AChE and BuChE *in vitro*

The inhibitory activities against AChE (from *electric eel*) and BuChE (from *Equine serum*) were measured by the Ellman's method.[32] Rivastigmine and donepezil were used as the reference compounds.[33,34] The results were summarized in Table 2.

As our expected, compounds **5a-5e** without the carbamate group have almost no inhibition of AChE and BuChE at a concentration of 20 μM. Compounds **6a-6f** with the introduction of carbamates on the hydroxyl group of **5a-5e**, have an increased inhibitory capacity of both AChE and BuChE. To our surprise, most compounds displayed good inhibitory activities against BuChE, with IC_{50} values ranging from 0.96 to 18.8 μM, while the inhibition against AChE at 20 μM were only between 17% to 28%. These results indicated that compounds **6a-6f** were selective BuChE inhibitors. As is mentioned in the introduction, the level of butyrylcholinesterase remained the same or even increased up to 2-fold while the level of acetylcholinesterase decreased in the advanced AD stage. Dual inhibitors of both AChE and BuChE or selective inhibitors of BuChE may be more suitable for therapy advanced AD patients.

Both the substituted groups on the phenyl ring and the configuration at the R position have effects on the inhibitory activities. Among compounds **6a-6e** with *N, N*-methylethyl carbamate group, compound **6c** with the 3-methoxyl and 4-carbamate group gave the best IC_{50} of BuChE (3.3 μM). The two stereisomers **6d** and **6e**, showed the IC_{50} of BuChE 3.7 and 17.9 μM, respectively, implying that the

difference in configurations plays an important role in the inhibition of BuChE. Compound **6f** with *N, N*-dimethyl carbamate groups at 4-position was also synthesized and evaluated, showing a better inhibitory activity (0.96 μM) than compound **6c** (3.3 μM). Both are more potent than current drugs rivastigmine (2.8 μM) and donepezil (8.1 μM). The selectivities of compounds **6c** and **6f** (BuChE/AChE) are above 7-fold and 20-fold, respectively. It is worthy to mention that compounds **6c** and **6f** also exhibited remarkable inhibitory affinity towards PDE9A with the IC_{50} of 14 and 17 nM, respectively. These are in accordance with our aim at designing dual inhibitors of PDE9A and cholinesterase.

The inhibition of AChE and BuChE by compounds **13a** and **13b** were also tested. Among all the designed compounds with carbamate groups, these two compounds showed the highest BuChE inhibitory activities, with the IC_{50} of 0.27 and 0.57 μM respectively, which was 10-fold and 6-fold than that of rivastigmine. The selectivity of compound **13a** (BuChE/AChE) could be up to 100. Although the low inhibition against PDE9A limited them to be dual inhibitors of PDE9A and cholinesterase, structural evidence provided by these two compounds may be useful for further modification.

2.5. Antioxidant activity by the ORAC method.

Oxidative stress has been considered as an important factor in the AD onset and progression. The oxidative damage caused by ROS and RNS may accelerate the aggregation of amyloid plaques in AD patients.[35, 36] Thus, antioxidants have been widely applied in the MTDLS for AD treatment. Hydroxyl-phenyl motif existed in many antioxidants such as resveratrol, ferulic acid and has been regarded as the pharmacophore for their antioxidant activities.[37,38] Oxygen radical absorbance capacity assay (ORAC-FL) is a widely applied method to test the antioxidant activities of hydrophilic antioxidants including phenolic derivatives. As compounds **5a-5e** with good inhibition against PDE9A contained a hydroxyl-phenyl motif, antioxidant activities of these compounds were evaluated by ORAC-FL method. The results were summarized in Table 2. As expected, all these compounds have good antioxidant activities,

with ORAC-FL values ranging from 0.9-1.8 Trolox equivalents. Compound **5d**, with the best IC_{50} value of 13 nM against PDE9A, gave an ORAC value of 1.0 Trolox. Compound **5c**, with a relatively lower IC_{50} value of 35 nM against PDE9A, gave the best ORAC value of 1.8 Trolox, which is even more active than the reference compound ferulic acid (1.1). These results indicated that compounds **5d** and **5c** were potent PDE9A inhibitors with antioxidant activities.

2.6. Inhibition of $A\beta_{1-42}$ self-aggregation by ThT assay.

One important hallmarks in the AD patients is amyloid beta (Aβ) aggregation.[39] Polyphenols, such as caffeic acid, feurlic acid have been reported that could inhibit Aβ self-aggregation.[40] Thus, a ThT fluorescence assay was performed on the designed compounds to evaluate their effects on $A\beta_{1-42}$ self-aggregation. The results were shown in Table 2. Compounds **5a, 5b, 6a,** and **6b** were able to inhibit Aβ self-aggregation to some extent at the concentration of 50 μM. Compound **5a** containing a hydroxyl group, gave a comparable activity (80%) to that of curcumin, a positive compound widely used for the evaluation of Aβ self-aggregation.

2.7. The selectivity of compounds 5d and 6c over PDEs.

The PDE enzyme superfamily are encoded with 21 genes and divided into 11 families according to the difference in structure and distribution. However, the binding pockets of some PDEs subfamilies are quite similar. Thus, PDE inhibitor may target at more than one PDE protein simultaneously, resulting in low selectivity. As each PDE subfamily is distributed differently and involved in different biological process, low selectivity over other PDEs may cause severe drug adverse effects and limit clinical usage. Thus, compounds **5d** and **6c**, with high IC_{50} against PDE9A (**5d**: 13 nM, **6c**: 14 nM) were choose to explore the selectivities over PDE1A, PDE4A, PDE5A and PDE8A. The results were shown in table 3. For the PDE9A inhibitors, selectivities over PDE1A and PDE8A are usually difficult to be obtained.[23-25]

Compounds **5d** and **6c** showed the selectivities of 8 and 9 over PDE1A, respectively. These results were almost the same as **C33**. In our previous report, we found that the interaction with Tyr424 in the binding pocket of PDE9A was important for high selectivity over other PDEs. The crystal of the **C33**-PDE9 complex revealed that **C33** didn't form the interaction with Tyr424 but entered into a small selective pocket, resulting in its moderate selectivity over PDE1A. Thus, we speculated that both compounds **5d** and **6c** didn't form the hydrogen bond with Tyr424, either. Furthermore, PDE8A protein contains a tyrosine residue at the corresponding Tyr424 position of PDE9A, the interaction with tyrosine residue might result in the low selectivity over PDE8A. In our tests, the selectivities of compounds **5d** and **6c** over PDE8A could get up to 700. This results further supported our speculation that compounds **5d** and **6c** didn't form the hydrogen bond with Tyr424. The inhibition ratio of **5d** at 1μM and 10μM is 29% and 84%, respectively, while that of 6c is 27% and 81%, respectively. Thus, the selectivites of compounds **5d** and **6c** over PDE4D were above 77 folds. The selectivities of compounds **5d** and **6c** over PDE5A were also evaluated, the selectivities of compound 5d over PDE5A is 8 folds and that of **6c** is 3 folds. Combined with these results, we concluded that both **5d** and **6c** were selective PDE9A inhibitors.

2.6. Effects of test compounds on the cell viability

The toxicity of compounds **5c, 5d, 6c** and **6f** were evaluated by using cell viability assays on the SH-SY5Y cell line (Figure 2). For compound **5c** with moderate IC_{50} against PDE9A and best antioxidant activity (1.8), the cell viability were 37% and 85% at 100 μM and 40 μM, respectively. For compound **5d** with the best IC_{50} against PDE9A and antioxidant activity(1.0), the cell viability were 70% and 97% at 100 μM and 40 μM, respectively. For compound **6c**, the dual inhibitor of PDE9A and BuChE, the cell viability were 53% and 83% at 100 μM and 40 μM, respectively. For compound **6f**, the other dual inhibitor of PDE9A and BuChE, the cell viability is 58% and 79% at 100 μM and 40 μM, respectively.

These results indicated that all these inhibitors we obtained were almost non-toxicity and suitable for further exploration.

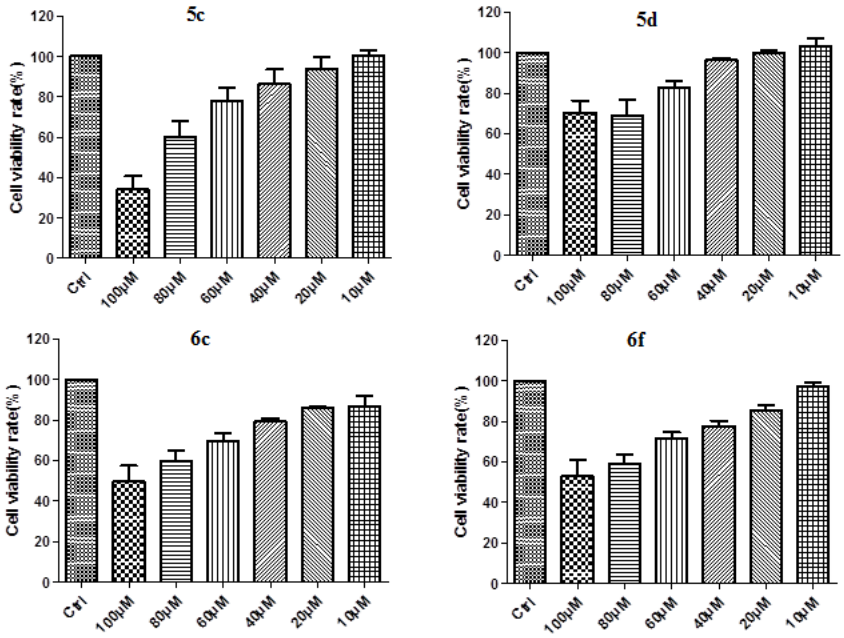

Figure 2. Cell viability in SH-SY5Y cells of compounds **5c, 5d**, **6c** and **6f**

2.7. Molecular modeling studies on the PDE9A-inhibitor complexes.

For compounds **5d** and **6c**, which showed the best IC_{50} value against PDE9A of 13 and 14 nM, respectively, molecular docking studies were performed to explore their binding modes with PDE9A. Furthermore, in order to explain the influence on affinity towards PDE9 caused by chiral conformation of inhibitors, binding modes of compounds **5e**, **6d**, and **6e** were also investigated.

In the binding pocket of PDE9A, Gln453 and Phe456 are two key residues for the affinity of inhibitor with PDE9A. As shown in Figure 3, compound **6c** formed an additional hydrogen bond with the key residue Gln453 besides two common hydrogen bonds with Gln453 and π-π stack with Phe456, resulting in its high affinity of PDE9A. The phenyl tail of two stereoisomers **5d** and **5e** entered into a small pocket of PDE9 protein like **C33** (Figure 4A, C, and E), but stretched to a different position

because of chiral configuration. The hydroxyl group on the compound **5d** with *R* configuration, formed an additional hydrogen bond with Ala452 beside the two hydrogen bonds with Gln453 whereas compound **5e** not. This might be the main reason that **5d** with *R* configuration gave better affinity of PDE9 than **5e** with *S* configuration.

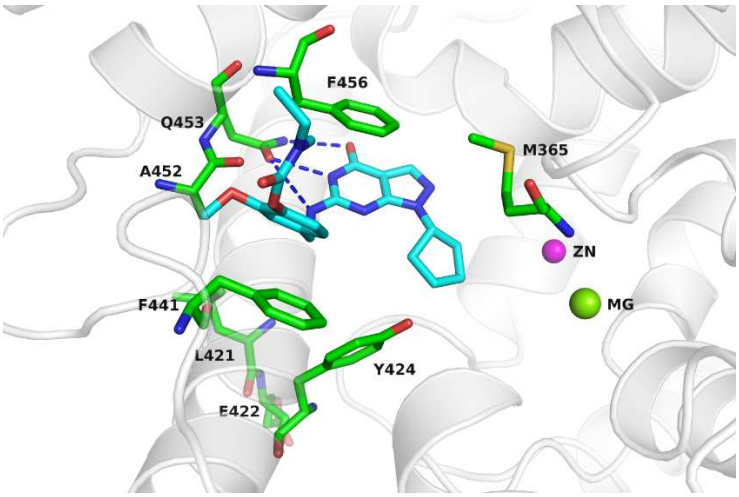

Figure 3: The binding mode of compound **6c** with PDE9A

After the carbamate groups were attached on the hydroxyl groups of **5d** and **5e,** forming the corresponding **6d** and **6e**, the influence on affinities caused by chiral configuration disappeared. Observed from the binding modes, compounds **6d** and **6e** adopted a similar binding mode (Figure 4B, D, and F), forming two hydrogen with Gln453 and an additional hydrogen bond with Ala452 *via* the nitrogen atom on the linker. However, dislike compounds **5d** and **5e**, the tail of compounds **6d** and **6e** switched to another position due to the steric hindrance of carbamate groups, forming a face to edge π-π interaction with Phe456. Thus, compounds **6d** and **6e** gave a comparable IC_{50} value against PDE9A.

For the compound **13a** and **13b**, which showed low inhibitory activities toward PDE9A, molecular docking method was adopted in the same way but could not obtain an appropriate configuration of complexes between **13a** or **13b** and PDE9A. The volume of side chains attached on the

pyrazolopyrimidinone ring of **13a** and **13b** were too large to enter the binding pocket of PDE9A, resulting in their low inhibitory activities.

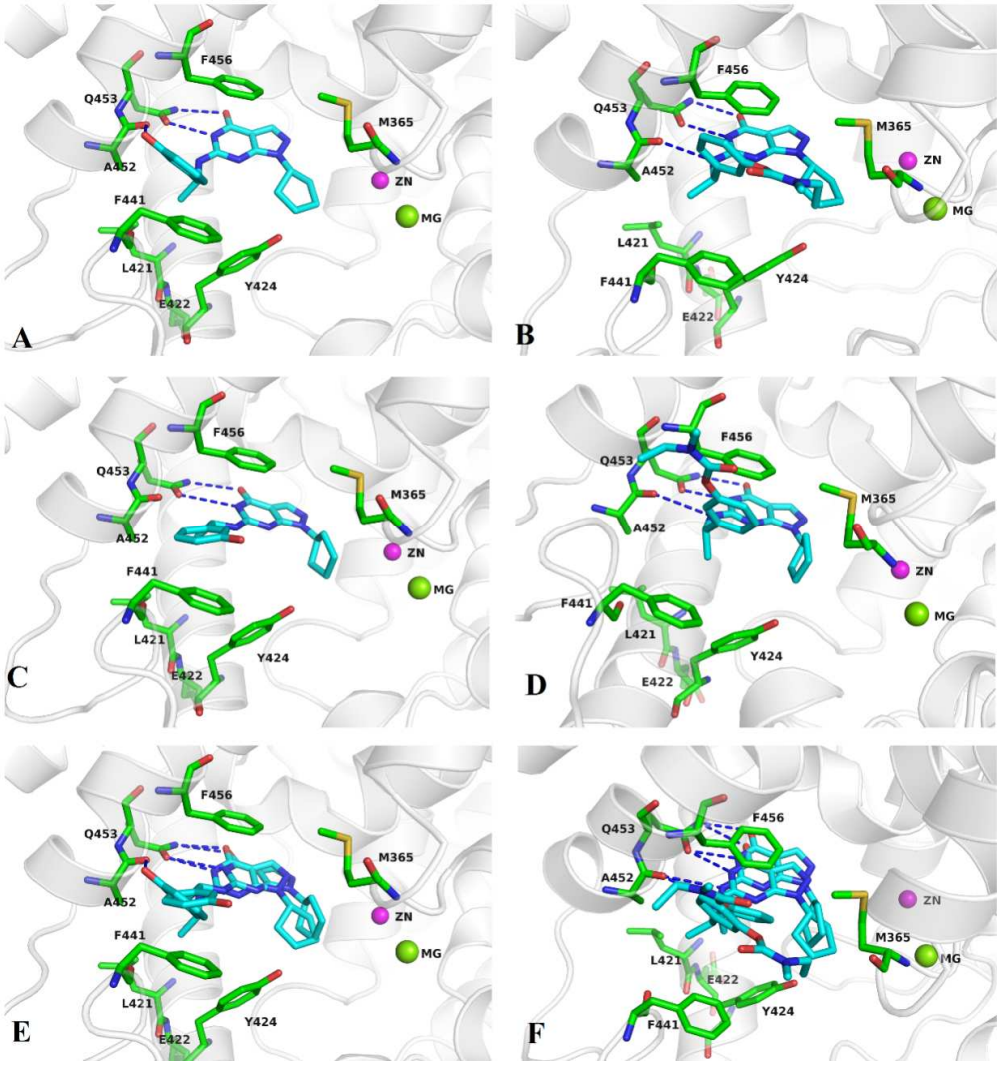

Figure 4: The binding mode of compounds **5d, 5e, 6d,** and **6e** with PDE9A protein. A) **5d**-PDE9A; B) **6d**-PDE9A; C) **5e**-PDE9A; D) **6e**-PDE9A; E) **5d+5e**-PDE9A; F) **6d+6e** -PDE9A

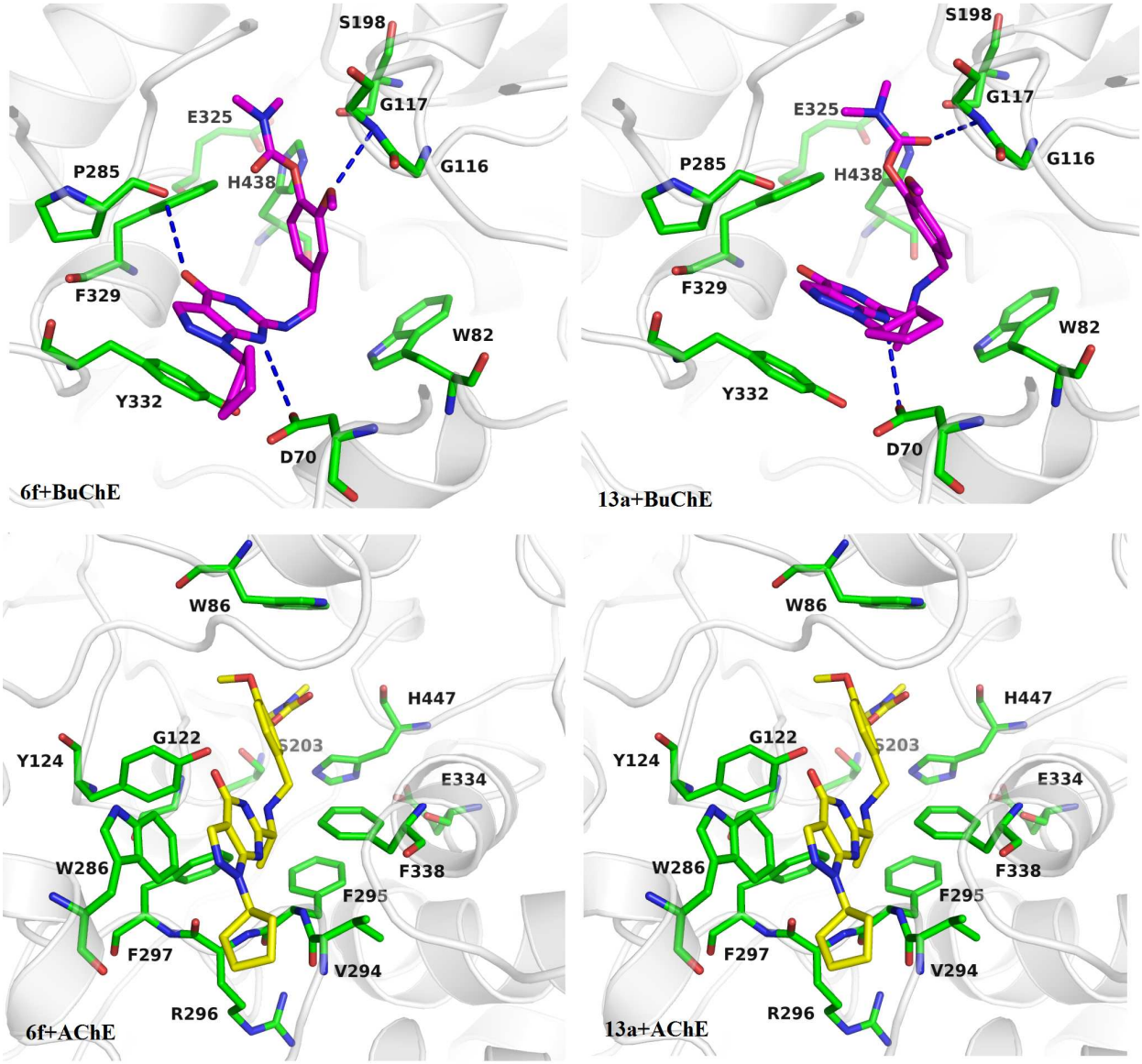

Figure 5: The binding patterns of compounds **6f** and **13a** with the AChE and BuChE.

2.8. Molecular modeling studies on the ChE-inhibitor complexes.

The binding modes of compounds **6f** and **13a** with AChE and BuChE were investigated by molecular docking, in order to explore the underlying mechanism for their high selectivity of BuChE over AChE. As shown in Figure 5, compounds **6f** and **13a** adopted similar binding modes. The carbamate group of

them inserted the catalytic domain of AChE and BuChE, forming van der Waals interactions with key amino residues Ser203, Glu334, and His447 in AChE and Ser198, Glu325, and His438 in BuChE, respectively. The pyrazolopyrimidinone motif formed π-π stacking interactions with Trp286 in AChE and Tyr332 in BuChE, respectively. However, two relative large amino residue Phe295 and Phe297 existed in the binding pocket of AChE, which made the mid-gorge site of AChE relatively small. The tail of compounds **6f** and **13a** could not fit well in this area. This might be the possible reason for the high selectivities of **6f** and **13a** over AChE.

The binding free energies of compound **13a**, which showed the best IC_{50} of 0.27 μM against BuChE and selectivity above100 over AChE, was calculated by the MM-PBSA method (Table 4).[41] The calculation results were in accordance with our experimental results. The absolute binding free energy of **13a**-BuChE was higher than that of **13a**-AChE. Electrostatic components (ΔG_{ele}) played a key role in the binding of **13a** with AChE and so did van der Waals (ΔG_{vdw}) in the binding of **13a** with BuChE. In addition, it was clearly visible that non-polar component to solvation ($\Delta G_{nonpol,\ solv}$) values was an unfavorable factor for the binding of **13a** with both AChE and BuChE.

3. Conclusion

In conclusion, a series of novel pyrazolopyrimidinone-rivastigmine hydrids were designed, synthesized, and evaluated in *vitro*. Most designed compounds exhibited dual inhibitory activities towards both PDE9A and BuChE. Compounds **6c** and **6f**, sharing a similar structure, were identified to be the most efficient ones. Both of them showed excellent inhibitory activities against PDE9A (**6c**: 14 nM and **6f**: 17 nM) and also were highly selective inhibitors towards BuChE (**6c**: 3.3 μM; **6f**: 0.97 μM). As a result, the inhibitory potency against BuChE and selectivity of BuChE/AChE of **6f** are much higher than current drug rivastigmine. Molecular docking studies were performed to explore structure-activity relationship of these compounds, which revealed the detailed binding modes and influence on inhibitory

activities caused by configurations. Cell viability assay in the SH-SY5Y cell line showed that both **6c** and **6f** have negligible toxicity, being worthy to be further explored in *vivo* study of AD.

4. Experimental section

4.1. Chemistry

Unless otherwise mentioned, all reagents were purchased from commercial suppliers and used without purification. Thin layer chromatography was performed on precoated silica gel 60 F_{254} plates. Silica gel (230-400 mesh) was used for column chromatography. ^{1}H NMR spectra were recorded on a 400 MHz spectrometer. Spectra were referenced internally to the residual proton resonance in $CDCl_3$ (δ 7.26 ppm) as the internal standard. Chemical shifts (δ) were reported as part per million (ppm) in δ scale downfield from TMS. ^{13}C NMR spectra were recorded on a 100 MHz spectrometer and the spectra were referenced to $CDCl_3$ (δ 77.0 ppm, the middle peak). Coupling constants (*J*) were reported in Hertz (Hz). High-resolution mass spectra (HRMS) were obtained on a LT-TOF.

4.1.1. General for the preparation of compound 5a-5e.

To the solution of intermediate **4** in *i*-propanol (2.0 mL), the corresponding amine (0.4 mmol) and trimethylamine (4 mg, 0.4 mmol) were added. The mixture was stirred at 80 ^{o}C for 1 hour. After the intermediate **4** was disappeared on the TLC, the solvent was removed by evaporation. The residue was purified on column chromatography (CH_2CI_2: MeOH=50:1) to give the compounds **5a-5e** in good yield.

4.1.2. 1-cyclopentyl-6-((3-hydroxybenzyl)amino)-1H-pyrazolo[3,4-d]pyrimidin-4(5H)-one (5a)

It was synthesized with 3-(aminomethyl)phenol as the starting material. Elution with methanol and dichloromethane (1:50) afforded compound **5a** (0.20 g, 61%) as a white solid.^{1}H NMR (400 MHz, DMSO) δ 10.48 (s, 1H), 7.75 (s, 1H), 7.13 (t, *J* = 7.8 Hz, 1H), 6.98 (s, 1H), 6.78 (d, *J* = 7.4 Hz, 2H), 6.65 (dd, *J* = 7.0, 1.4 Hz, 1H), 4.97 - 4.88 (m, 1H), 4.45 (d, *J* = 5.7 Hz, 2H), 2.02 - 1.80 (m, 6H), 1.62 (dd, *J* = 9.9, 4.8 Hz, 2H). ^{13}C NMR (101 MHz, MeOD) δ 157.55, 133.83, 129.10, 118.06, 114.06,

113.84, 99.75, 57.61, 44.28, 31.27, 24.24. HRMS (ESI-TOF) m/z [M + H]+calcd for C_{17} H_{19} N_5 O_2 326.1612 , found 326.1605 .

4.1.3. 1-cyclopentyl-6-((3-hydroxy-4-methoxybenzyl)amino)-1H-pyrazolo[3,4-d]pyrimidin -4(5H) -one (5b)

It was synthesized with 5-(aminomethyl)-2-methoxyphenol as the starting material. Elution with methanol and dichloromethane (1:50) afforded compound **5b** (0.19 g, 53%) as a white solid. ^{1}H NMR (400 MHz, DMSO) δ 8.93 (s, 1H), 7.74 (d, *J* = 1.7 Hz, 1H), 6.87 (d, *J* = 8.2 Hz, 1H), 6.86 - 6.79 (m, 2H), 6.76 (dd, *J* = 8.2, 2.1 Hz, 1H), 4.99- 4.91 (m, 1H), 4.38 (d, *J* = 5.6 Hz, 2H), 3.74 (s, 3H), 2.08- 1.79 (m, 8H), 1.70 - 1.59 (m, 2H). ^{13}C NMR (101 MHz, DMSO) δ 158.25, 154.02, 153.56, 147.32, 146.93, 134.31, 131.84, 118.89, 115.57, 112.62, 100.20, 57.14, 56.16, 44.04, 32.14, 24.78. HRMS (ESI-TOF) m/z [M + H]+calcd for C_{18} H_{21} N_5 O_3 356.1717, found 356.1708.

4.1.4. 1-cyclopentyl-6-((4-hydroxy-3-methoxybenzyl)amino)-1H-pyrazolo[3,4-d]pyrimidin -4(5H)-one (5c)

It was synthesized with 4-(aminomethyl)-2-methoxyphenol as the starting material. Elution with methanol and dichloromethane (1:50) afforded compound **5c** (0.17 g, 49%) as a white solid.^{1}H NMR (400 MHz, $CDCl_3$) δ 11.01 (s, 1H), 7.52 (s, 1H), 6.88 (d, *J* = 8.7 Hz, 3H), 6.44 (t, *J* = 5.3 Hz, 1H), 5.97 (s, 1H), 5.07 - 5.01 (m, 1H), 4.56 (d, *J* = 5.3 Hz, 2H), 3.80 (s, 3H), 2.07 (dd, *J* = 7.2, 5.0 Hz, 4H), 1.98 - 1.92 (m, 2H). ^{13}C NMR (101 MHz, Acetone) δ 205.31, 205.11, 133.65, 120.66, 114.83, 111.73, 57.19, 55.42, 44.54, 31.74, 29.46, 29.26, 29.07, 28.88, 28.69, 28.50, 28.30, 24.47. HRMS (ESI-TOF) m/z [M + H]+calcd for C_{18} H_{21} N_5 O_3 356.1717, found 356.1717.

4.1.5. (*R*)-1-cyclopentyl-6-((1-(3-hydroxyphenyl)ethyl)amino)-1H-pyrazolo[3,4-d]pyrimidin -4(5H)-one (5d)

It was synthesized with (*R*)-3-(1-aminoethyl)phenol as the starting material. Elution with methanol and dichloromethane (1:50) afforded compound **5d** (0.27 g, 68%) as a white solid.^{1}H NMR (400 MHz, $CDCl_3$) δ 7.76 (s, 1H), 7.14 (d, *J* = 7.8 Hz, 1H), 7.05 (s, 1H), 6.94 (s, 1H), 6.87 (d, *J* = 7.5 Hz, 1H), 6.75 (d, *J* = 7.9 Hz, 1H), 5.20 - 5.11 (m, 1H), 4.90 (s, 1H), 2.06 - 2.00 (m, 3H), 1.95 (dd, *J* = 13.1, 6.3 Hz, 3H), 1.65 (d, *J* = 6.3 Hz, 2H), 1.52 (d, *J* = 6.8 Hz, 3H). ^{13}C NMR (101 MHz, MeOD) δ 161.19, 158.72, 155.59, 153.63, 147.00, 135.23, 130.58, 118.11, 115.02, 114.05, 101.04, 59.39, 52.06, 32.66, 32.44, 25.63, 25.59, 22.85. HRMS (ESI-TOF) m/z [M + H]+ calcd for C_{18} H_{21} N_5 O_2 340.1768, found 340.1763.

4.1.6. (*S*)-1-cyclopentyl-6-((1-(3-hydroxyphenyl)ethyl)amino)-1H-pyrazolo[3,4-d]pyrimidin -4(5H)-one (5e)

It was synthesized with (*S*)-3-(1-aminoethyl)phenol as the starting material. Elution with methanol and dichloromethane (1:50) afforded compound **5e** (0.17 g, 49%) as a white solid.^{1}H NMR (400 MHz, $CDCl_3$) δ 7.72 (s, 1H), 7.13 (d, *J* = 7.5 Hz, 1H), 7.04 (dd, *J* = 17.8, 9.9 Hz, 2H), 6.82 (d, *J* = 7.6 Hz, 1H), 6.73 (dd, *J* = 8.0, 1.7 Hz, 1H), 5.08 (s, 1H), 4.90 - 4.83 (m, 1H), 2.00 - 1.90 (m, 4H), 1.87 - 1.80 (m, 2H), 1.60 (dd, *J* = 6.5, 5.2 Hz, 2H), 1.47 (d, *J* = 6.9 Hz, 3H). ^{13}C NMR (101 MHz, $CDCl_3$) δ 161.06, 156.94, 154.17, 151.69, 144.99, 133.98, 129.89, 117.90, 114.89, 112.26, 99.49, 58.00, 49.81, 31.69, 31.46, 29.32, 24.67, 24.60, 21.77. HRMS (ESI-TOF) m/z [M + H]+calcd for C_{18} H_{21} N_5 O_2 340.1768, found 340.1761.

4.1.7. General for the preparation of compound 6a-6f.

To the solution of compound **5** (1.0 mmol) in DMF (15 mL), sodium hydride (4.8 mg, 2.0 mmol) and *N,N*-ethyl(methyl)carbamic chloride (0.25 g, 2.0 mmol) were added subsequently. The mixture was stirred at room temperature for 1h. The mixture was then extracted with dichloromethane three times. The combined organic layer was washed with water three times, dried over sodium sulfate and

evaporated to afford the crude product. The crude product was purified by column chromatography to afford the compound **6** as a colorless solid.

4.1.8. 3-(((1-cyclopentyl-4-oxo-4, 5-dihydro-1H-pyrazolo[3,4-d]pyrimidin-6-yl)amino)methyl) phenyl ethyl(methyl)carbamate (6a)

It was synthesized with compound **5a** as the starting material. Elution with methanol and dichloromethane (1:100) afforded compound **6a** (0.30 g, 73%) as a white solid.^{1}H NMR (400 MHz, $CDCl_3$) δ 10.47 (d, *J* = 14.6 Hz, 1H), 7.82 - 7.72 (m, 1H), 7.32 (t, *J* = 7.8 Hz, 1H), 7.19 - 7.09 (m, 2H), 7.01 (d, *J* = 5.1 Hz, 1H), 6.43 (d, *J* = 46.7 Hz, 1H), 4.98 (p, *J* = 7.6 Hz, 1H), 4.56 (d, *J* = 5.5 Hz, 2H), 3.44 (dq, *J* = 26.6, 7.1 Hz, 2H), 3.00 (t, *J* = 20.7 Hz, 3H), 2.09 - 2.01 (m, 4H), 1.94 - 1.88 (m, 2H), 1.79 (dd, *J* = 10.8, 5.6 Hz, 2H), 1.68 (dt, *J* = 8.9, 3.9 Hz, 2H), 1.27 - 1.17 (m, 3H). ^{13}C NMR (101 MHz, $CDCl_3$) δ 160.07, 152.68, 151.63, 140.12, 134.39, 129.47, 121.01, 114.29, 100.10, 57.47, 44.51, 31.92, 24.75, 13.27, 12.57. HRMS (ESI-TOF) m/z [M + H]+calcd for C_{21} H_{26} N_6 O_3 411.2139, found 411.2146.

4.1.9. 5-(((1-cyclopentyl-4-oxo-4, 5-dihydro-1H-pyrazolo[3,4-d]pyrimidin-6-yl)amino)methyl) -2-methoxyphenyl ethyl(methyl)carbamate (6b)

It was synthesized with compound **5b** as the starting material. Elution with methanol and dichloromethane (1:100) afforded compound **6b** (0.29 g, 66%) as a white solid. ^{1}H NMR (400 MHz, $CDCl_3$) δ 10.20 (s, 1H), 8.01 (s, 1H), 7.81 (s, 1H), 7.11 (d, *J* = 7.3 Hz, 2H), 6.88 (d, *J* = 8.5 Hz, 1H), 6.41 (s, 1H), 5.00 (p, *J* = 7.4 Hz, 1H), 4.47 (d, *J* = 5.3 Hz, 2H), 3.80 (s, 3H), 3.48 (dd, *J* = 14.0, 7.0 Hz, 1H), 3.39 (dd, *J* = 14.0, 6.9 Hz, 1H), 2.96 (s, 3H), 2.88 (s, 3H), 2.04 (s, 6H), 1.98 - 1.87 (m, 3H), 1.73 - 1.64 (m, 2H), 1.25 (t, *J* = 6.9 Hz, 3H), 1.17 (dd, *J* = 15.5, 8.5 Hz, 2H). ^{13}C NMR (101 MHz, $CDCl_3$) δ 159.83, 154.84, 154.66, 154.17, 152.76, 151.00, 140.50, 140.42, 134.39, 130.88, 125.59, 125.53, 122.76, 122.70, 112.40, 112.34, 100.07, 100.01, 99.99, 57.39, 56.04, 44.32, 44.14, 34.43, 33.96, 31.95, 24.84,

24.77, 12.94, 12.37. HRMS (ESI-TOF) m/z [M + H]+calcd for C_{22} H_{28} N_6 O_4 441.2245, found 441.2241.

4.1.10. 4-(((1-cyclopentyl-4-oxo-4, 5-dihydro-1H-pyrazolo[3,4-d]pyrimidin-6-yl) amino) methyl) -2-methoxyphenyl ethyl(methyl) carbamate (6c)

It was synthesized with compound **5c** as the starting material. Elution with methanol and dichloromethane (1:100) afforded compound **6c** (0.24 g, 54%) as a white solid.^{1}H NMR (400 MHz, $CDCl_3$) δ 10.36 (s, 1H), 7.81 (s, 1H), 7.02 (dd, *J* = 8.0, 4.5 Hz, 1H), 6.84 (s, 1H), 6.80 (d, *J* = 8.0 Hz, 1H), 6.15 (s, 1H), 5.00 - 4.95 (m, 1H), 4.50 (d, *J* = 5.6 Hz, 2H), 3.78 (s, 3H), 3.49 (dt, *J* = 17.5, 7.1 Hz, 2H), 3.11 (s, 2H), 3.03 (s, 2H), 2.07 - 2.02 (m, 4H), 1.92 (dd, *J* = 13.4, 9.3 Hz, 2H), 1.29 - 1.25 (m, 3H), 1.21 (t, *J* = 7.1 Hz, 2H).^{13}C NMR (101 MHz, $CDCl_3$) δ 159.95, 154.15, 152.79, 151.67, 139.68, 136.86, 134.26, 123.14, 119.43, 111.60, 100.09, 99.98, 57.52, 55.95, 44.59, 44.31, 34.43, 31.93, 24.74, 12.90, 12.34. HRMS (ESI-TOF) m/z [M + H]+calcd for C_{22} H_{28} N_6 O_4 441.2245, found 441.2246.

4.1.11. (*R*)-3-(1-((1-cyclopentyl-4-oxo-4, 5-dihydro-1H-pyrazolo[3,4-d]pyrimidin-6-yl) amino) ethyl) phenyl ethyl(methyl)carbamate (6d)

It was synthesized with compound **5d** as the starting material. Elution with methanol and dichloromethane (1:100) afforded compound **6d** (0.24 g, 56%) as a white solid.^{1}H NMR (400 MHz, $CDCl_3$) δ 10.40 (s, 1H), 7.77 - 7.74 (m, 1H), 7.30 (t, *J* = 7.8 Hz, 1H), 7.19 (dd, *J* = 11.0, 5.7 Hz, 2H), 7.00 (s, 1H), 6.72 (d, *J* = 8.7 Hz, 1H), 5.19 (p, *J* = 6.6 Hz, 1H), 4.95 (p, *J* = 7.6 Hz, 1H), 3.41 (dq, *J* = 25.0, 7.1 Hz, 2H), 3.00 (d, *J* = 32.2 Hz, 3H), 2.10 - 1.98 (m, 5H), 1.98 - 1.88 (m, 3H), 1.73 - 1.63 (m, 2H), 1.59 (d, *J* = 6.9 Hz, 3H), 1.19 (dt, *J* = 16.9, 7.1 Hz, 3H). ^{13}C NMR (101 MHz, $CDCl_3$) δ 160.14, 154.24, 151.91, 151.61, 134.20, 129.40, 123.03, 120.70, 119.75, 100.01, 57.69, 50.23, 44.13, 34.28, 33.84, 31.90, 31.76, 24.77, 24.75, 22.25, 13.21, 12.47. HRMS (ESI-TOF) m/z [M + H]+calcd for C_{22} H_{28} N_6 O_3 425.2296, found 425.2298.

4.1.12. (*S*)-3-(1-((1-cyclopentyl-4-oxo-4, 5-dihydro-1H-pyrazolo[3,4-d]pyrimidin-6-yl)amino) ethyl)phenyl ethyl(methyl) carbamate(6e)

It was synthesized with compound **5e** as the starting material. Elution with methanol and dichloromethane (1:100) afforded compound **6e** (0.262 g, 62%) as a white solid.^{1}H NMR (400 MHz, $CDCl_3$) δ 7.81 (s, 1H), 7.34 (d, *J* = 7.9 Hz, 1H), 7.25 - 7.19 (m, 2H), 7.03 (s, 1H), 6.56 (d, *J* = 6.7 Hz, 1H), 5.25 - 5.18 (m, 1H), 4.98 (dd, *J* = 15.2, 7.6 Hz, 1H), 3.50 - 3.38 (m, 2H), 3.07 (s, 1H), 2.98 (s, 2H), 2.12 - 2.02 (m, 4H), 1.97 - 1.90 (m, 2H), 1.69 (td, *J* = 6.6, 3.2 Hz, 2H), 1.61 (d, *J* = 6.9 Hz, 3H), 1.27 - 1.18 (m, 3H). ^{13}C NMR (101 MHz, $CDCl_3$) δ 151.84, 134.26, 77.33, 77.01, 76.69, 57.70, 50.28, 31.89, 31.77, 24.74, 22.14. HRMS (ESI-TOF) m/z [M + H]+calcd for $C_{22}H_{28}N_6O_3$ 425.2296, found 425.2299.

4.1.13. 4-(((1-cyclopentyl-4-oxo-4,5-dihydro-1H-pyrazolo[3,4-d]pyrimidin-6-yl)amino) methyl) - 2-methoxyphenyl dimethylcarbamate (6f)

It was synthesized with compound **5c** as the starting material. Elution with methanol and dichloromethane (1:100) afforded compound **6f** (0.242 g, 57%) as a white solid.^{1}H NMR (400 MHz, $CDCl_3$) δ 10.38 (s, 1H), 7.75 (s, 1H), 7.01 (d, *J* = 8.0 Hz, 1H), 6.87 (d, *J* = 1.7 Hz, 1H), 6.82 (dd, *J* = 8.1, 1.8 Hz, 1H), 6.41 (t, *J* = 5.6 Hz, 1H), 4.98 (p, *J* = 7.6 Hz, 1H), 4.51 (d, *J* = 5.6 Hz, 2H), 3.77 (s, 3H), 3.13 (s, 3H), 3.02 (s, 3H), 2.05 (dd, *J* = 13.0, 5.9 Hz, 4H), 1.96 - 1.86 (m, 2H), 1.70 - 1.61 (m, 2H). ^{13}C NMR (101 MHz, $CDCl_3$) δ 159.94, 155.23, 154.12, 152.78, 151.63, 139.53, 136.95, 134.34, 123.16, 119.33, 111.40, 100.10, 57.42, 55.95, 44.53, 36.94, 36.63, 31.98, 24.78. HRMS (ESI-TOF) m/z [M + H]+calcd for $C_{21}H_{26}N_6O_4$ 427.2088, found 427.2093.

4.1.14. General for the preparation of compound 13a-13b.

To a solution of intermediated **12** (0.12 g, 0.5 mmol) in DMF(5.0 mL), sodium borohydride (34 mg, 0.8 mmol) and aldehyde (0.8 mmol) were added at 0 ^{o}C. The mixture was stirred for 30 min at room temperature. Water (15 mL) was added. The mixture was extracted with ethyl acetate three times. The combined organic layer was washed with brine, dried over anhydrous sodium sulfate, and evaporated to give crude product. The crude product was purified by column chromatography to afford the compound **13** as a colorless solid.

4.1.15. (*R*)-5-(((1-(1-cyclopentyl-4-oxo-4,5-dihydro-1H-pyrazolo[3,4-d]pyrimidin-6-yl)ethyl) amino)methyl)-2-methoxyphenyl dimethylcarbamate (13a)

It was synthesized with 4-formyl-2-methoxyphenyl dimethylcarbamate as the starting material. Elution with methanol and dichloromethane (1:100) afforded compound **13a** (0.22 g, 48%) as a white solid. ^{1}H NMR (400 MHz, $CDCl_3$) δ 10.17 (s, 1H), 8.08 (s, 1H), 7.06 (d, *J* = 7.9 Hz, 1H), 6.93 - 6.85 (m, 2H), 5.25 - 5.13 (m, 1H), 3.87 (s, 3H), 3.81 - 3.68 (m, 2H), 3.14 (s, 3H), 3.03 (s, 3H), 2.12 (dd, *J* = 12.0, 6.2 Hz, 4H), 2.00 (dd, *J* = 13.3, 9.7 Hz, 2H), 1.77 - 1.72 (m, 2H), 1.48 (d, *J* = 6.8 Hz, 3H). ^{13}C NMR (101 MHz, $CDCl_3$) δ 161.67, 158.35, 154.73, 152.40, 151.80, 139.88, 137.06, 134.57, 123.35, 120.14, 112.25, 104.98, 57.79, 56.27, 56.04, 52.15, 36.80, 36.56, 32.47, 32.37, 24.75, 21.54. HRMS (ESI-TOF) m/z [M + H]+calcd for C_{23} H_{30} N_6 O 4455.2401, found 455.2402.

4.1.16. (*R*)-5-(((1-(1-cyclopentyl-4-oxo-4,5-dihydro-1H-pyrazolo[3,4-d]pyrimidin-6-yl)ethyl) amino)methyl)-2-methoxyphenyl ethyl(methyl)carbamate(13b)

It was synthesized with 4-formyl-2-methoxyphenyl ethyl(methyl)carbamate as the starting material. Elution with methanol and dichloromethane (1:100) afforded compound **13b** (0.18 g, 39%) as a white solid. ^{1}H NMR (400 MHz, $CDCl_3$) δ 10.29 (s, 1H), 8.08 (s, 1H), 7.05 (d, *J* = 7.9 Hz, 1H), 6.87 (dd, *J* = 8.9, 7.4 Hz, 2H), 5.18 (p, *J* = 7.5 Hz, 1H), 3.85 (s, 3H), 3.81 - 3.66 (m, 2H), 3.46 (dd, *J* = 32.5, 6.3 Hz, 2H), 3.05 (d, *J* = 38.6 Hz, 3H), 2.18 - 2.09 (m, 4H), 2.00 (dd, *J* = 12.6, 9.7 Hz, 2H), 1.78 - 1.72 (m, 2H),

1.47 (d, *J* = 6.8 Hz, 3H), 1.24 (d, *J* = 27.2 Hz, 3H). ^{13}C NMR (101 MHz, $CDCl_3$) δ 161.84, 158.62, 154.49, 154.31, 152.38, 151.76, 139.89, 139.80, 137.13, 134.54, 123.30, 120.13, 112.29, 112.21, 104.91, 57.76, 56.24, 55.94, 52.00, 44.22, 44.13, 34.33, 33.89, 32.45, 32.36, 26.89, 24.80, 24.74, 24.69, 21.48, 12.96, 12.40. HRMS (ESI-TOF) m/z [M + H]+calcd forC24 H32 N6 O4 469.2558, found 469.2560.

4.2. In *vitro* bioassay test for the inhibition of PDE9

The PDE9A2 protein was purified by the protocols according to our previous reports.[25] ^{3}H-cGMP as the substrate for the biological test against PDE9A2. ^{3}H-cGMP was diluted with the assay buffer which contained 20-50 mM Tris-HCl (pH 8.0),10 mM $MgCl_2$ and 1 mM DTT to 20 000-30 000 cpm per assay. And then, the reaction was performed at 25 ^{o}C for 15 min, which was terminated by the addition of 0.2 M $ZnSO_4$. After the addition of 0.2 N $Ba(OH)_2$, a precipitate was formed and the unreacted ^{3}H-cGMP left in the supernatant. The radioactivity in the supernatant was measured in 2.5 mL of Ultima Gold liquid scintillation cocktails (PerkinElmer) using a PerkinElmer 2910 liquid scintillation counter. For the measurement of IC_{50} of inhibitors, eight different concentrations were used and each measurement was repeated three times. The IC_{50} values against PDE9 were calculated by nonlinear regression. The mean values of the measurements were considered as the final IC_{50} values with the SD values of the measurements.

4.3. AChE/BuChE inhibition activity

The inhibition activity of designed compounds on *ee*AChE and *eq*BuChE were tested using the the Ellman's method.[32] Compounds were diluted using the enzyme buffer (0.1 M KH_2PO_4/K_2HPO_4 buffer, pH 8.0). The final concentration of 5, 5' -dithiobis (2-nitrobenzoic acid) was 0.25 M. The mixture was incubated with 0.25 unit of AChE at 37 ^{o}C for 15 min. After mixing with ATC (0.25 M), the mixture was scanned immediately at 412 nm using Thermo Scientific VarioskanFlash. The average absorbance variation for 5 consecutive minutes was calculated. The inhibitory rate for each compound was

calculated by comparing the average absorbance of samples containing compounds with the absence of test compounds. The dose-response curve and concentration for inhibit 50% enzyme activity (IC_{50}) was calculated in GraphPad version 5 by fitting replicates with the lg(inhibitor) vs normalized response variable slope equation. The BuChE test was performed in the same procedure with BTC as the substrate for BuChE

4.4. The ORAC test for the antioxidant activities

The antioxidant activity was tested using the modified oxygen radical absorbance capacity fluorescein (ORAC-FL) method [42,43]. Each assays was diluted with phosphate buffer (75 mM, pH 7.4) to make the final reaction mixture 200 μL. Test compound (20 μL) and fluorescein (120 μL, 150 nM final concentration) were placed in the wells of a black 96-well plate. The mixture was then incubated at 37 ^{o}C for 15 min. AAPH solution (60 μL, 12 mM) was added rapidly. The fluorescence of this plate was recorded every minute for 4h with excitation at 485 nm and emission at 535 nm in a Spectrafluor Plus plate reader (Tecan, Crailsheim, Germany). Trolox was used as standard. All the reaction mixture was prepared at least three independent assays were performed. The ORAC-FL values were expressed as Trolox equivalents.

4.4. In vitro cell viability assay

SH-SY5Y cells was used for the cytotoxicity test by using the MTT (3-(4, 5-dimethyl-2- thiazolyl)-2,5-diphenyl -2-H-tetrazolium bromide) method.[44] The SH-SY5Y cells (5×10^3) were inoculated into a 96-well plate. After 24 h, compounds at the concentration of 10 μM, 20 μM, 40 μM, 60 μM, 80 μM and 100 μM, were added. After incubation for 48 h, MTT solution was added to each cell well and inoculated for 4 h at 37 ^{o}C. After the purple formazan dye was dissolved, 100 μL DMSO was added to the cells. The absorbance of each cell well was measured at 570 nm using Flex Station 3 (Molecular Devices).

4.5. Molecular docking and MD simulations for PDE9A

The X-ray crystal structure of **28**-PDE9A complex (PDB ID: 4GH6) reported in our previous studies[25] was selected for molecular modeling. Surflex-dock[45] embedded in the software Tripos Sybyl 2.0 was used. Two metal ions crucial for the PDE's catalytic activity in the catalytic domain and water molecules coordinate these two metal ions were retained. Hydrogen atoms were added, and the ionizable residues were protonated at the neutral pH. The protomol, was generated using the parameters by default. The parameters of proto_thresh and proto_bloat were assigned 0.5 and 0, respectively. After the protomol was the prepared, molecular docking was performed for test molecules.

After molecular docking was completed, MD simulations were used to equilibrate the whole system. 8 ns MD simulations were performed after minimization, heating and equilibration steps of each system. The 100 snapshots were isolated from the final 1.0 ns period of the MD simulation trajectories, and then used for binding-free-energy calculations by the MM-PBSA approach[46-48].

The PBSA program in the Amber 16[49], which could numerically solves the PoissoneBoltzmann equations, was used to calculate the electrostatic contribution to the solvation-free energy. MM-PBSA binding free energy (ΔG_{bind}) calculations were performed by the extraction of 100 snapshots of the last 1 ns trajectories by equation 1 using default parameters. $G_{complex}$, G_{rec} and G_{lig} represent the free energies of complex, receptor and ligand, respectively. Each free energy was evaluated by the sum of the MM energy E_{MM}, the solvation free energy G_{solv}, and the entropy contribution S, respectively, leading to equation 2.

$$\Delta G_{bind} = G_{complex} - G_{rec} - G_{lig} \qquad (1)$$

$$\Delta G_{bind} = \Delta E_{MM} + \Delta G_{solv} - T\Delta S \qquad (2)$$

ΔE_{MM} is the gas phase interaction energy and can be decomposed into $E_{MM,\,comp}$, $E_{MM,\,rec}$ and $E_{MM,\,lig}$. Solvation free energy is evaluated by the sum of the electrostatic solvation free energy and nonpolar solvation free energy. The electrostatic solvation free energy, ΔG_{PB}, was solved by the Poisson

Boltzmann (PB) equation, while the nonpolar solvation free energy varies proportionally with the solvation accessible surface area (SASA), leading to by equation 3 and 4

$$\Delta G_{solv} = \Delta G_{PB} + \Delta G_{np} \quad (3)$$

$$\Delta G_{np} = \gamma \, SASA + b \quad (4)$$

Although entropy contribution term can be evaluated by the normal mode analysis, the process is extremely time-consuming for large protein-ligand systems. In order to get the compromise between efficiency and accuracy, entropy contribution term was omitted for ΔG_{bind} in equation (2). The default parameters were adopted, with γ = 0.0072 kcal/(Å^2) and b = 0 kcal/mol.The charges of Mg^{2+} and Zn^{2+} were assigned 2.0 for PB calculations, and their bond raddi were used for SA calculations.

4.6 Molecular docking and MD simulations for AChE and BuChE

The crystal structures of human AChE and BuChE with bound inhibitors (PDB ID: 4EY7 and 4TPK) were used for molecular docking, respectively. The residues of each receptor was protonated in pH of 7.0 and atoms' partial charges were assigned by the CHARMm force field. The docking site was defined as spheres with a 8 Å radius covering the binding site. CDOCKER protocol embedded in Discovery Studio 2.5 was utilized for docking of **6f** and **13a** to AChE and BuChE. The other docking parameters were set by default. Twenty top-ranked docking poses were retained and carefully analyzed. The most appropriate pose was retained and was subjected to MD simulations. 8 ns MD simulations were performed and 100 snapshots were isolated from the final 2 ns of the trajectory for the following binding-free-energy calculations using the MM-PBSA method in the Amber 16 with the same procedure in 4.5.

■ ASSOCIATED CONTENT

Supporting Information

^{1}H and ^{13}C NMR spectra of compounds **5a-5e, 6a-6f** and **13a-13b.** The Supporting Information is available free of charge on the ACS Publications website.

■ AUTHOR INFORMATION

Corresponding Authors

* E-mail: wyinuo3@mail.sysu.edu.cn (Y.W)

* E-mail: luohb77@mail.sysu.edu.cn; Fax: +86-20-3994 3000 (H.B.L.).

ORCID

Yinuo Wu: 0000-0003-3071-5333

Hai-Bin Luo: 0000-0002-2163-0509

Author Contributions

Y. F. Yu and Y. D. Huang contributed equally to this work. Y. F. Yu, X. N. Wu and D. Wu performed the synthetic work. Y. D. Huang and Q. Zhou performed the biological test. C. Zhang performed molecular docking and dynamic simulation calculation. Y. Wu and H.-B. Luo designed the studies and wrote the manuscript.

Funding

This work was supported by the National Key R&D Program of China (2017YFB0202600), Natural Science Foundation of China (81522041, 81373258, 21572279, 21402243, and 81602968), Science Foundation of Guangdong Province (2014A020210009 and 2016A030310144), Guangdong Province Higher Vocational Colleges & Schools Pearl River Scholar Funded Scheme (2016), Foundation of Traditional Chinese medicine Bureau of Guangdong Province (20171049) and State Key Laboratory for Chemistry and Molecular Engineering of Medicinal Resources (CMEMR2016-B03). We thank Special

Program for Applied Research on Super Computation of the NSFC-Guangdong Joint Fund (the second phase) under Grant No.U1501501 for providing the supercomputing service.

Notes

The authors declare no competing financial interest.

■Acknowledgements

We cordially thank Prof. H. Ke from Department of Biochemistry and Biophysics at the University of North Carolina, Chapel Hill, for his help with molecular cloning, expression, purification, crystal structure, and bioassay of PDEs.

Reference:

1. Stopschinski, B. E., and Diamond, M. I. (2017) The prion model for progression and diversity of neurodegenerative diseases. *Lancet Neurol., 16*(4), 323-332.
2. Alzheimer's Association (USA). World Alzheimer Report 2015, http://news.medlive.cn/uploadfile/20150902/14411602338388.pdf.
3. Goedert, M., and Spillantini, M. G. (2006) A century of Alzheimer's disease. *Science, 314*(5800), 777-781.
4. Bartus, R. T., Dean, R. L., 3rd, Beer, B., and Lippa, A. S. (1982) The cholinergic hypothesis of geriatric memory dysfunction. *Science, 217*(4558), 408-414.
5. Herrmann, N., Chau, S. A., Kircanski, I., and Lanctot, K. L. (2011) Current and Emerging Drug Treatment Options for Alzheimer's Disease A Systematic Review. *Drugs, 71*(15), 2031-2065.
6. Nordberg, A., Ballard, C., Bullock, R., Darreh-Shori, T., and Somogyi, M. (2013) A review of butyrylcholinesterase as a therapeutic target in the treatment of Alzheimer's disease. *Prim Care Companion CNS Disord., 15*(2), PCC.12r01412.

7. Darvesh, S., Hopkins, D. A., and Geula, C. (2003) Neurobiology of butyrylcholinesterase. *Nat. Rev. Neurosci., 4*(2), 131-138.
8. Reyes-Irisarri, E., Ittersum, M. M. V., Mengod, G., and de Vente, J. (2007) Expression of the cGMP-specific phosphodiesterases 2 and 9 in normal and Alzheimer's disease human brains. *Eur. J. Neurosci., 25*(11), 3332-3338.
9. Garcia-Osta, A., Cuadrado-Tejedor, M., Garcia-Barroso, C., Oyarzabal, J., and Franco, R. (2012) Phosphodiesterases as Therapeutic Targets for Alzheimer's Disease. *ACS Chem. Neurosci., 3*(11), 832-844.
10. van der Staay, F. J., Rutten, K., Barfacker, L., Devry, J., Erb, C., Heckroth, H., Karthaus, D., Tersteegen, A., van Kampen, M., Blokland, A., Prickaerts, J., Reymann, K. G., Schroder, U. H., and Hendrix, M. (2008) The novel selective PDE9 inhibitor BAY 73-6691 improves learning and memory in rodents. *Neuropharmacology, 55*(5), 908-918.
11. Hutson, P. H., Finger, E. N., Magliaro, B. C., Smith, S. M., Converso, A., Sanderson, P. E., Mullins, D., Hyde, L. A., Eschle, B. K., Turnbull, Z., Sloan, H., Guzzi, M., Zhang, X., Wang, A., Rindgen, D., Mazzola, R., Vivian, J. A., Eddins, D., Uslaner, J. M., Bednar, R., Gambone, C., Le-Mair, W., Marino, M. J., Sachs, N., Xu, G., and Parmentier-Batteur, S. (2011) The selective phosphodiesterase 9 (PDE9) inhibitor PF-04447943 (6-[(3S,4S)-4-methyl-1-(pyrimidin-2-ylmethyl)pyrrolidin-3-yl]-1-(tetrahydro-2H-pyran-4-yl)-1,5-dihydro-4H-pyrazolo[3,4-d]pyrimidin-4-one) enhances synaptic plasticity and cognitive function in rodents. *Neuropharmacology, 61*(4), 665-676.
12. Kroker, K. S., Rast, G., Giovannini, R., Marti, A., Dorner-Ciossek, C., and Rosenbrock, H. (2012) Inhibition of acetylcholinesterase and phosphodiesterase-9A has differential effects on hippocampal early and late LTP. *Neuropharmacology, 62*(5-6), 1964-1974.
13. Kleiman, R. J., Lanz, T. A., Finley, J. E.,; Bove, S. E., Majchrzak, M. J., Becker, S. L., Carvajal-Gonzales, S., Kuhn, A. M., Wood, K. M., Mariga, A., Nelson, F. R., Verhoest, P. R., Seymour, P.

A., Stephenson, D. T. (2010) Dendritic spine density deficits in the hippocampal CA1 region of young Tg2576 mice are ameliorated with the PDE9A inhibitor PF-04447943. *Alzheimer's & Dementia, 6* (4), 563-564.

14. Kroker, K. S., Mathis, C., Marti, A., Cassel, J. C., Rosenbrock, H., and Dorner-Ciossek, C. (2014) PDE9A inhibition rescues amyloid beta-induced deficits in synaptic plasticity and cognition. *Neurobiol. Aging, 35*(9), 2072-2078.
15. Li, J., Liu, C. N., Wei, N., Li, X. D., Liu, Y. Y., Yang, R., and Jia, Y. J. (2016) Protective effects of BAY 73-6691, a selective inhibitor of phosphodiesterase 9, on amyloid-beta peptides-induced oxidative stress in in-vivo and in-vitro models of Alzheimer's disease. *Brain Research, 1642*, 327-335.
16. Rosini, M., Simoni, E., Caporaso, R., and Minarini, A. (2016) Multitarget strategies in Alzheimer's disease: benefits and challenges on the road to therapeutics. *Future Med. Chem., 8*(6), 697-711.
17. Sameem, B., Saeedi, M., Mahdavi, M., and Shafiee, A. (2017) A review on tacrine-based scaffolds as multi-target drugs (MTDLs) for Alzheimer's disease. *Eur. J. Med. Chem., 128*, 332-345.
18. Weinreb, O., Amit, T., Bar-Am, O., and Youdim, M. B. H. (2012) Ladostigil: A Novel Multimodal Neuroprotective Drug with Cholinesterase and Brain-Selective Monoamine Oxidase Inhibitory Activities for Alzheimer's Disease Treatment. *Curr. Drug Targets, 13*(4), 483-494.
19. Bolognesi, M. L., Cavalli, A., and Melchiorre, C. (2009) Memoquin: A Multi-Target-Directed Ligand as an Innovative Therapeutic Opportunity for Alzheimer's Disease. *Neurotherapeutics, 6*(1), 152-162.
20. Vanmierlo, T., Creemers, P., Akkerman, S., van Duinen, M., Sambeth, A., De Vry, J., Uzd, T., Bloklandc, A. and Prickaerts, J. (2016). The PDE4 inhibitor roflumilast improves memory in rodents at non-emetic doses. *Behav. Brain Res.*, *303*, 26-33.

21. Arai, H. and Takahashi, T. (2009) A combination therapy of donepezil and cilostazol for patients with moderate Alzheimer disease: pilot follow-up study. *Am. J. Geriatr. Psychiatry.,17* (4),353-354.

22. Huang, M. N., Shao, Y. X., Hou, J. Y., Cui, W. J., Liang, B. B., Huang, Y. C., Li, Z., Wu, Y. N., Zhu, X. H., Liu, P. Q., Wan, Y. Q., Ke, H. M., and Luo, H. B. (2015) Structural Asymmetry of Phosphodiesterase-9A and a Unique Pocket for Selective Binding of a Potent Enantiomeric Inhibitor. *Mol. Pharmaco., 88*(5), 836-845.

23. Claffey, M. M., Helal, C. J., Verhoest, P. R., Kang, Z. J., Fors, K. S., Jung, S., Zhong, J. Y., Bundesmann, M. W., Hou, X. J., Lui, S. P., Kleiman, R. J., Vanase-Frawley, M., Schmidt, A. W., Menniti, F., Schmidt, C. J., Hoffman, W. E., Hajos, M., McDowell, L., O'Connor, R. E., MacDougall-Murphy, M., Fonseca, K. R., Becker, S. L., Nelson, F. R., and Liras, S. (2012) Application of Structure-Based Drug Design and Parallel Chemistry to Identify Selective, Brain Penetrant, In Vivo Active Phosphodiesterase 9A Inhibitors. *J. Med. Chem., 55*(21), 9055-9068.

24. DeNinno, M. P., Andrews, M., Bell, A. S., Chen, Y., Eller-Zarbo, C., Eshelby, N., Etienne, J. B., Moore, D. E., Palmer, M. J., Visser, M. S., Yu, L. J., Zavadoski, W. J., and Gibbs, E. M. (2009) The discovery of potent, selective, and orally bioavailable PDE9 inhibitors as potential hypoglycemic agents. *Bioorg. Med. Chem. Lett., 19*(9), 2537-2541.

25. Meng, F., Hou, J., Shao, Y. X., Wu, P. Y., Huang, M. N., Zhu, X. H., Cai, Y. H., Li, Z., Xu, J., Liu, P. Q., Luo, H. B., Wan, Y. Q., and Ke, H. M. (2012) Structure-Based Discovery of Highly Selective Phosphodiesterase-9A Inhibitors and Implications for Inhibitor Design. *J. Med. Chem., 55*(19), 8549-8558.

26. Gottwald, M. D., and Rozanski, R. I. (1999) Rivastigmine, a brain-region selective acetylcholinesterase inhibitor for treating Alzheimer's disease: review and current status. *Expert Opin. Investig. Drugs, 8*(10), 1673-1682.

27. Bullock, R. (2002) The clinical benefits of rivastigmine may reflect its dual inhibitory mode of action: An hypothesis. *Int. J. Clin. Pract., 56*(3), 206-214.

28. Bolognesi, M. L., Bartolini, M., Cavalli, A., Andrisano, V., Rosini, M., Minarini, A., and Melchiorre, C. (2004) Design, synthesis, and biological evaluation of conformationally restricted rivastigmine analogues. *J. Med. Chem., 47*(24), 5945-5952.

29. Su, T., Zhang, T. H., Xie, S. S., Yan, J., Wu, Y., Li, X. S., Huang, L., and Luo, H.-B. (2016) Discovery of novel PDE9 inhibitors capable of inhibiting A beta aggregation as potential candidates for the treatment of Alzheimer's disease. *Sci. Rep., 6*. 20836

30. Li, Z., Lu, X., Feng, L. J., Gu, Y., Li, X. S., Wu, Y, and Luo, H.-B. (2015) Molecular dynamics-based discovery of novel phosphodiesterase-9A inhibitors with non-pyrazolopyrimidinone scaffolds. *Mol. Biosyst., 11*(1), 115-125.

31. Wunder, F., Tersteegen, A., Rebmann, A., Erb, C., Fahrig, T., and Hendrix, M., (2005) Characterization of the first potent and selective PDE9 inhibitor using a cGMP reporter cell line. *Mol. Pharmacol. 68* (6), 1775-1781.

32. Ellman, G. L., Courtney, K. D., Andres, V., Jr., and Feather-Stone, R. M. (1961) A new and rapid colorimetric determination of acetylcholinesterase activity. *Biochem. Pharmaco., 7*, 88-95.

33. Wang, Y. L., Sun, Y., Guo, Y. Y., Wang, Z. C., Huang, L., and Li, X. S. (2016) Dual functional cholinesterase and MAO inhibitors for the treatment of Alzheimer's disease: synthesis, pharmacological analysis and molecular modeling of homoisoflavonoid derivatives. *J. Enzyme Inhib. Med. Chem., 31*(3), 389-397.

34. Sang, Z., Pan, W., Wang, K., Ma, Q., Yu, L., and Liu, W. (2017) Design, synthesis and biological evaluation of 3, 4-dihydro-2(1H)-quinoline-O-alkylamine derivatives as new multipotent cholinesterase/monoamine oxidase inhibitors for the treatment of Alzheimer's disease. *Bioorg. Med. Chem., 25*(12), 3006-3017.

35. Tailor, N., and Sharma, M. (2013) Antioxidant hybrid compounds: a promising therapeutic intervention in oxidative stress induced diseases. *Mini-Rev. Med. Chem., 13*(2), 280-297.

36. Zhang, H. Y., Yang, D. P., and Tang, G. Y. (2006) Multipotent antioxidants: from screening to design. *Drug Discovery Today, 11* (15-16), 749-754.

37. Mohamed, T., and Rao, P. P. N. (2017) 2,4-Disubstituted quinazolines as amyloid-beta aggregation inhibitors with dual cholinesterase inhibition and antioxidant properties: Development and structure-activity relationship (SAR) studies. *Eur. J. Med. Chem., 126*, 823-843.

38. Sang, Z. P., Pan, W. L., Wang, K. R., Ma, Q. G., Yu, L. T., Yang, Y., Bai, P., Leng, C. L., Xu, Q., Li, X. Q., Tan, Z. H., and Liu, W. M. (2017) Design, synthesis and evaluation of novel ferulic acid-O-alkylamine derivatives as potential multifunctional agents for the treatment of Alzheimer's disease. *Eur. J. Med. Chem., 130*, 379-392.

39. Mohamed, T., Shakeri, A., and Rao, P. P. N. (2016) Amyloid cascade in Alzheimer's disease: Recent advances in medicinal chemistry. *Eur. J. Med. Chem., 113*, 258-272.

40. Huang, H., Ma, Z. C., Wang, Y. G., Hong, Q., Tan, H. L., Xiao, C. R., Liang, Q. D., Tang, X. L., and Gao, Y. (2015) Ferulic acid alleviates $Abeta_{25-35}$- and lipopolysaccharide-induced PC12 cellular damage: a potential role in Alzheimer's disease by PDE inhibition. *Int. J. Clin. Pharmacol. Ther., 53*(10), 828-837.

41. Wang, L., Wang, Y., Tian, Y., Shang, J., Sun, X., Chen, H., Wang, H., and Tan, W., (2017) Design, synthesis, biological evaluation, and molecular modeling studies of chalcone-rivastigmine hybrids as cholinesterase inhibitors. *Bioorg. Med. Chem., 25* (1), 360-371.

42. Ou, B., Hampsch-Woodill, M., and Prior, R. L. (2001). Development and validation of an improved oxygen radical absorbance capacity assay using fluorescein as the fluorescent probe. *J. Agric. Food. Chem., 49*(10), 4619-4626.

43. Dávalos, A., Gómez-Cordovés, C., and Bartolomé, B. (2004). Extending applicability of the oxygen radical absorbance capacity (ORAC− fluorescein) assay. *J. Agric. Food. Chem., 52*(1), 48-54.

44. Encinas, M., Iglesias, M., Liu, Y., Wang, H., Muhaisen, A., Cena, V., Gallego, C., and Comella, J. X. (2000). Sequential treatment of SH−SY5Y cells with retinoic acid and brain-derived neurotrophic factor gives rise to fully differentiated, neurotrophic factor-dependent, human neuron−like cells. *J. Neurochem.*, *75*(3), 991-1003.

45. Jain, A. N. (2003) Surflex: Fully automatic flexible molecular docking using a molecular similarity-based search engine. *J. Med. Chem., 46*(4), 499-511.

46. Massova, I., and Kollman, P. A. (2000) Combined molecular mechanical and continuum solvent approach (MM-PBSA/GBSA) to predict ligand binding. *Perspect. Drug Discov., 18*, 113-135.

47. Hou, T. J., Wang, J. M., Li, Y. Y., and Wang, W. (2011) Assessing the Performance of the MM/PBSA and MM/GBSA Methods. 1. The Accuracy of Binding Free Energy Calculations Based on Molecular Dynamics Simulations. *J. Chem. Inf. Model., 51*(1), 69-82.

48. Xu, L., Sun, H. Y., Li, Y. Y., Wang, J. M., and Hou, T. J. (2013) Assessing the Performance of MM/PBSA and MM/GBSA Methods. 3. The Impact of Force Fields and Ligand Charge Models. *J. Phys. Chem. B, 117*(28), 8408-8421.

49. Case, D. A., et al. AMBER 16, University of California, San Francisco, (2014).

Table 1. The inhibitory activities of compounds **5a-5e** and **6a-6f** against PDE9A**.**

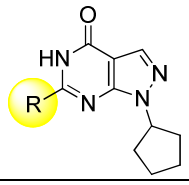

Compound	R	IC_{50}+SD (nM)[a]	Compound	R	IC_{50}+SD (nM)[a]
5a	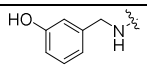	53±1	**6a**	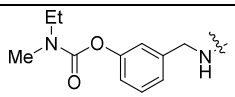	19±1
5b	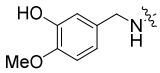	39±1	**6b**	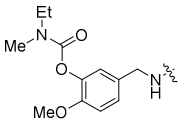	32±1
5c	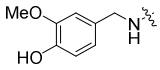	35±2	**6c**	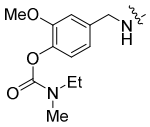	14±2
5d	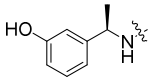	13±1	**6d**	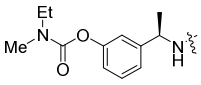	37±4
5e	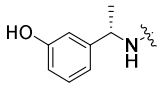	69±3	**6e**	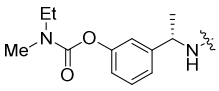	30±2
13a	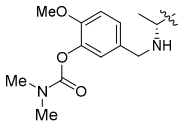	23.14%[b]	**6f**	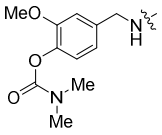	17±4
13b	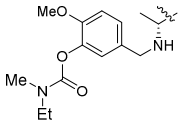	19.77%[b]	**Bay73-6691**	-	51[c]
C33	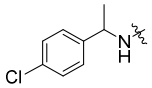	16±4[d]	**C10**	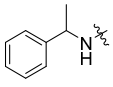	39±15[d]
(*R*)-C33	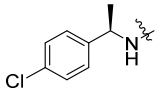	58±2[d]	**(*S*)-C33**	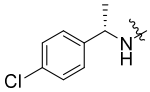	11±4[d]

[a] IC_{50} values are given as the mean of three independent determinations.

[b] Inhibition rates at 100 nM. [c] The IC_{50} value reported in the literature is 55 nM.[31]

[d] IC_{50} values from our previous work.[22]

Table 2. The inhibitory activities towards AChE and BuChE, ORAC activity and $A\beta_{1-42}$ self-aggregation inhibition of designed compounds *in vitro*.

Compound	$IC_{50} \pm SD$ (μM)[a]		Selectivity (BuChE/AChE)	ORAC	$A\beta_{1-42}$ self-aggregation inhibition
	*ee*AChE	*eq*BuChE			
5a	n.a.[b]	n.a.	-	0.9	80.43%[d]
5b	n.a.	n.a.	-	1.0	61.60%[d]
5c	n.a.	n.a.	-	1.8	n.a.
5d	n.a.	n.a.	-	0.9	n.a.
5e	n.a.	n.a.	-	1.0	17.55%[d]
6a	28.7%[c]	18.8±0.6	>1	-	67.94%[d]
6b	17.4%[c]	6.9±0.1	>3	-	48.86%[d]
6c	34.5%[c]	3.3±0.2	>7	-	n.a.
6d	23.9%[c]	3.7±0.1	>5	-	n.a.
6e	23.4%[c]	17.9±2.2	>1	-	n.a.
6f	5.34%[c]	0.96±0.18	>20	-	n.a
13a	52.6%[c]	0.27±0.04	≈74	-	n.a
13b	46.9%[c]	0.57±0.11	>40	-	n.a
Rivastigmine	3.28±0.06	2.89±0.15	0.9	-	-
Donepezil	0.024	8.14		-	-
Curcumin					80.12%

[a] IC_{50} values are given as the mean of three independent determinations.

[b] n.a. = no active. Compounds defined "no active" means a percent inhibition of less than 10.0% at a concentration of 20 μM.

[c] The inhibition against AChE at 20 μM.

[d] The measurements were carried out in the presence of 50 μM test compounds. The thioflavin-T fluorescence method was used.

Table 3. The selectivity of compounds **5d** and **6c** over PDE1 and PDE8.

Compound	IC_{50} (nM) of PDE9A	IC_{50} (nM) of PDE1A	IC_{50} (nM) of PDE4D	IC_{50} (nM) of PDE5A	IC_{50} (nM) of PDE8A
5d	13	100 (8)	> 1000 (> 77)	100 (8)	> 10000 (> 769)
6c	14	129 (9)	> 1000 (> 77)	39 (3)	> 10000 (> 714)
C33[b]	16	152 (9)	1800 (110)	197 (12)	1600 (98)

[a] The numbers in parentheses are the fold of selectivity of inhibitors against PDE9 over other PDEs.

[b] The data used here was obtained from our previous report.[22]

Table 4. Predicted binding free energies (kcal/mol) for binding of **13a** to human AChE and BuChE by the MM-PBSA method

Energy Terms (kcal/mol)	AChE	BuChE
ΔG_{ele}[a]	-19.39 ± 3.40	-8.95 ± 1.86
ΔG_{vdw}[b]	-53.78 ± 3.75	-57.60 ± 2.05
$\Delta G_{nonpol,sol}$[c]	11.10 ± 0.85	1.65 ± 0.13
$\Delta G_{ele,solc}$[d]	47.63 ± 5.76	39.90 ± 4.77
$\Delta G_{bind,pred}$[e]	-14.44 ± 4.42	-25.00 ± 5.01

[a] ΔG_{ele}, electrostatic interactions calculated using the MM force field.

[b] ΔG_{vdw}, van der Waals' contributions from MM.

[c] $\Delta G_{nonpol,\ sol,}$ the nonpolar contribution to solvation.

[d] $\Delta G_{ele.sol,}$ the polar contribution to solvation.

[e] $\Delta G_{bind,\ pred} = \Delta G_{ele} + \Delta G_{vdw} + \Delta G_{nonpol,\ sol} + \Delta G_{ele,\ sol,}$ the predicted binding free energies with the entropic contribution omitted.

Discovery of novel pyrazolopyrimidinone derivatives as PDE9A inhibitors capable of inhibiting BuChE for treatment of Alzheimer's disease

Yan-Fa Yu[‡,a] Ya-Dan Huang[‡,a] Chen Zhang,[a] Xu-Nian Wu,[a] Qian Zhou,[a] Deyan Wu,[a]

Yinuo Wu [a,*] and Hai-Bin Luo[a,b,*]

[a] School of Pharmaceutical Sciences, Sun Yat-Sen University, Guangzhou 510006, PR China

[b] Collaborative Innovation Center of High Performance Computing, National University of Defense Technology, Changsha 410073, China

[‡]These authors contributed equally.

Table of content graphic

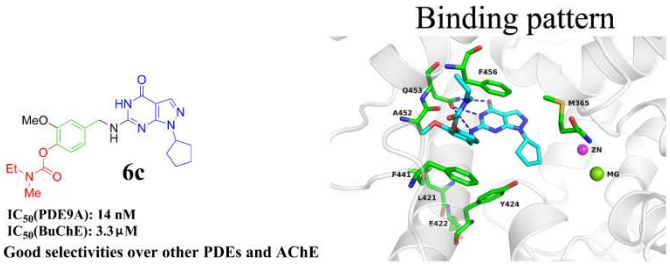

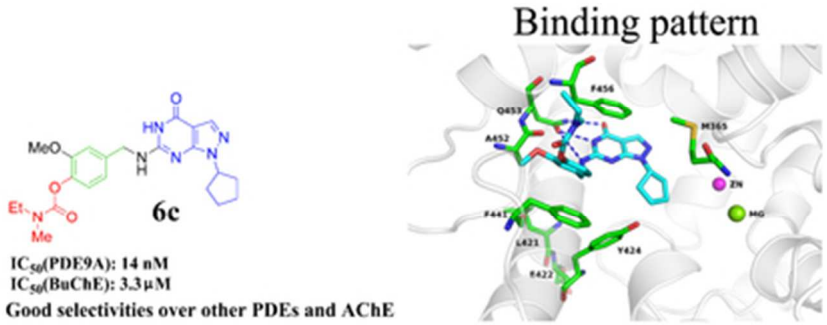

Table of content graphic

34x13mm (300 x 300 DPI)